X-651-72-101
PREPRINT

NASA TM X- 65996

IMPROVEMENT OF SYNOPTIC SCALE MOISTURE AND WIND FIELD ANALYSES USING THE NIMBUS 4 THIR 6.7μm OBSERVATIONS

JOSEPH STERANKA
LEWIS J. ALLISON
VINCENT V. SALOMONSON

APRIL 1972

GSFC — GODDARD SPACE FLIGHT CENTER —
GREENBELT, MARYLAND

X-651-72-101
PREPRINT

IMPROVEMENT OF SYNOPTIC SCALE MOISTURE AND WIND FIELD ANALYSES USING THE NIMBUS 4 THIR 6.7μm OBSERVATIONS

by

Joseph Steranka
Lewis J. Allison
Vincent V. Salomonson

Laboratory for Meteorology
and Earth Sciences

April 1972

GODDARD SPACE FLIGHT CENTER
Greenbelt, Maryland

IMPROVEMENT OF SYNOPTIC SCALE MOISTURE AND WIND FIELD ANALYSES USING THE NIMBUS 4 THIR 6.7 μm OBSERVATIONS

by

Joseph Steranka

Lewis J. Allison

Vincent V. Salomonson

Laboratory for Meteorology

and Earth Sciences

Goddard Space Flight Center

Greenbelt, Maryland 20771

ABSTRACT

The Nimbus 4 Temperature-Humidity Infrared Radiometer (THIR) monitors radiation in the 6.5-7.2 μm water vapor absorption with a 23 kilometer spatial resolution at the sub-satellite point. Radiation monitored in this spectral region results primarily from emission in the 250-500 millibar region of the upper troposphere. The THIR 6.7 μm observations are readily available in photofacsimile imagery form which shows very distinctive patterns associated with spatial variations in atmospheric water vapor.

These radiometric observations have been combined in several instances with moisture values measured in the upper troposphere by the standard radiosonde network. In each instance, the result is a much more consistent analysis

showing increased spatial detail that agrees with the radiometric observations and does not compromise the conventional data. The improved moisture analyses show relatively dry and moist tongues that are very difficult or impossible to infer from the conventional data alone. The patterns in the moisture fields can be tracked over 12 and 24 hour periods. In addition, by keeping in mind the advective properties of the moisture field, success has been achieved in improving streamline analyses at the 400 mb level over data sparse regions on a global scale.

CONTENTS

IMPROVEMENT OF SYNOPTIC SCALE MOISTURE AND WIND FIELD ANALYSES USING THE NIMBUS 4 THIR 6.7μm OBSERVATIONS

1. INTRODUCTION

In seeking to better understand and forecast the behavior of the atmosphere, meteorologists have been concerned with a lack of conventional meteorological data, particularly over the oceanic regions of the world. Since the flight of the first meteorological satellite, efforts have been made to interpret and apply these data so as to supplement ground-based meteorological observations. Reviews by Möller and Raschke (1969) and Shenk and Salomonson (1970) provide an overview of much of the progress that occurred in the first decade of satellite meteorology. As early as 1960 on TIROS II, radiometric observations were made in the spectral region near the 6.3 μm water vapor absorption region (Allison, 1964). These observations have been utilized to map relative humidity in the upper troposphere (Allison and Warnecke, 1965; Raschke and Bandeen, 1967) and to infer the location and extent of dynamic features in the upper troposphere (Nordberg, et al., 1966; Beran, et al., 1968; and Martin and Salomonson, 1970).

In many of the efforts above, much of the data analysis involved the processing of rather large amounts of digital data on high speed computers. This paper seeks to show that the relatively inexpensive and easily available imagery from radiometric observations in the 6.7 μm absorption region can be used in conjunction with quantitative conventional "benchmark" moisture and wind

observations. These satellite observations permit one to refine and improve the spatial detail in analyses of these parameters and to extend the analyses into regions where conventional observations are sparse or non-existent.

2. DATA DESCRIPTION

The Temperature-Humidity Infrared Radiometer (THIR) experiment flown aboard the Nimbus 4 meteorological satellite provided equivalent black-body temperature observations of cloud tops and the earth's surface with a 10.5-12.7 μm window channel and concurrent measurements of the moisture distribution in the upper troposphere (250-500 mb) with a 6.5-7.2 μm water vapor channel. The window channel and the water vapor channel had spatial resolutions at the subsatellite point of 8 and 23 kilometers, respectively. Photofacsimile imagery of the radiation data obtained from both channels are readily available from the NASA Space Science Data Center in Greenbelt, Maryland (McCulloch, 1970).

With respect to the water vapor channel, moisture rich or cloudy regions are indicated by the white or light grey shading on the imagery and the drier areas are delineated by dark grey to black tones. It is in regions where the window channel shows no cloudiness that the potential utility of the water vapor channel begins to appear. The water vapor channel, in clear sky situations, is not affected by the surface to any appreciable degree except over regions with high surface elevation or at high latitudes where the atmosphere is very dry and the surface very cold. Therefore, with the water vapor channel considerable

detail associated with the water vapor distribution is observed and outlined in the imagery. Fig. 1 illustrates the photofacsimile imagery of the window channel and water vapor channel. In area A on Fig. 1 a cloud mass exists and is visible in both channels. Areas B and C are clear or have only very thin cloudiness (Keegan, 1972), yet very noticeable detail delineating relatively dry and moderately moist regions can be seen in the water vapor channel.

3. RESULTS

(a) Water Vapor Analysis

Before one proceeds to apply the THIR 6.7 μm imagery for any purpose, it should be emphasized that the level or the vertical extent of the moisture producing the grey shades in the imagery is only very broadly defined as being commonly between the 500-250 mb levels. The contribution function, ψ that applies for the Nimbus 4 THIR 6.7 μm channel as it would appear when applied to a standard atmosphere, is shown in Fig. 2(a). The relative spectral response of the Nimbus 4 THIR 6.7 μm channel is shown in Fig. 2(b). One can see that significant portions of the response occur below 500 mb and above 250 mb. Furthermore, this contribution function will distort and/or move up or down as the amount and vertical distribution of the temperature and moisture in the middle and upper troposphere changes. An analysis of the existing vertical moisture distribution of a total of 58 radiosonde soundings at 15 mid-latitude stations and 1 tropical station, in relation to the grey shades in the 6.7 μm imagery, indicates that an experienced analyst can make a subjective judgement of the relative

vertical stratification of the moisture content. An abbreviated description of the interpretation guidelines commonly applied to each of the different grey shades is given in Table 1. Therefore some care must be exercised in applying the results to any particular level.

Table 1

Grey Shade (6.7μ m imagery)	Relative Moisture Distribution
Dark or Very Light Grey	Dry at all levels or moist only in the levels near the surface
Moderate Grey	Dry at intermediate levels (700 to 500 mb), moist above and/or below
Bright White	Moist at all levels*

Computation of the contribution function for a wide variety of typical soundings at various latitudes indicates that the range in the level from which the principal contribution arises is approximately 3 km at a given station in the mid-latitudes. This same range is somewhat larger in the tropics (4 - 5 km) and approximately one-half as much (1 - 2 km) in the polar latitudes. The height of the mean contribution level goes from about 8 km in the tropics to near 4 km in the polar latitudes.

The interpretative problems just described are counterbalanced by the fact that these water vapor observations give contiguous and synoptic coverage with relatively high spatial resolution over large areas. This paper seeks to

*Dense high and middle clouds can also give a bright white shade in the 6.7 μm imagery.

demonstrate that it is possible to utilize the patterns in the imagery to supplement and refine conventional "benchmark" observations made at conventional radiosonde stations. For this purpose the patterns shown in Fig. 1 have been utilized to draw an improved 400 millibar mixing ratio analysis for 1200 Z on October 16, 1970. The 400 millibar level was selected because it is the closest standard pressure level to the level (350-400 mb) where the maximum contribution to the emitted radiances observed by the water vapor channel is believed to occur. Due consideration has been given to the difference in time between water vapor channel observations and the conventional and radiosonde observations.

The analyzed moisture chart for the 400 mb level using only the conventional observations is shown in Fig. 3(a). This analysis was done by an experienced analyst having full cognizance of the flow patterns and the general meteorological events occurring within the map area. Fig. 3(b) is an analysis for the same level and time, but in this case the general configuration in the moisture patterns agree with the water vapor channel observations. Numerous differences and/or improvements are evident in Fig. 3(b) when compared to Fig. 3(a). Point A and B illustrates that improved positioning and delineation of a moderate moisture region has occurred. Point C shows that the analysis can be more definitely extended into a no-data region. Point D shows that the water vapor channel observations leads one to connect the high moisture region over Texas with the high moisture region over New England. Point E shows that the water vapor channel dictates that a region of low moisture extending east-west should

be drawn. The water vapor channel observations also permit more detail in the water vapor distribution over Eastern Canada to be drawn than is suggested by the conventional observations alone. It should be explicitly noted that the conventional observations have not been violated or altered in the improved analysis shown in Fig. 3(b). Overall, the improved analysis provides a definition of patterns that cannot be made with the conventional data alone. The water vapor channel is clearly providing an observational basis for extrapolating the conventional measurements into data-void regions.

(b) Wind Field

A qualitative comparison of the moisture patterns on the 6.7μm imagery with the 400 mb level conventionally measured wind field also indicates that the moisture patterns are generally aligned with the wind field. This suggests that the water vapor imagery could be used to infer the orientation of streamlines over data sparse regions. Fig. 4 shows a streamline analysis derived from water vapor channel imagery taken over the Western United States. The direction applied to the streamline analysis requires knowledge of circulation patterns within meteorological systems such as low and high pressure areas. Particular caution must be exercised in frontal regions with high, dense cloudiness since frontal clouds are often not aligned with the upper tropospheric wind flow. This analysis procedure has been applied with some appreciable success over other areas and the general experience to date indicates that this procedure provides a definite and valuable guide for improving wind flow analyses over the oceanic regions of the world. An example of a global analysis will be discussed in the next section.

(c) Application of 6.7 μm Observations to Improved Moisture and Wind Flow Analyses on a Global Scale

In order to more completely describe the potential use of the 6.7 μm observations, the types of analysis described in Fig. 3 and 4 have been extended spatially to cover most of the globe on 16 October 1970. The composite of the photofacsimile film strips (6.7 μm channel) Nimbus 4 THIR, orbits 2561 to 2574 (Night) 16 October 1970 is shown in Fig. 5. As an intermediate step in the preparation of an enhanced global moisture analysis, it was deemed judicious to translate the 5 shades of grey in Fig. 5 to a mercator projection (Fig. 6). Then, all available 400 mb moisture content data for 00 GMT, 16 and 17 October 1970 were plotted on the same map base. An enhanced global 400 mb moisture analysis was then derived by preserving to the greatest extent possible, the moisture distribution patterns in both sets of data (Fig. 7). One can note the overall agreement between the satellite patterns (Fig. 6) and those drawn from conventional data wherever it existed (Fig. 7).* As is well known, relatively few conventional radiosonde observations are available in the Southern Hemisphere. The 6.7 μm observations provide a substantive basis for extrapolating the conventional observations into the data-void oceanic regions, especially the tropics. Although this moisture analysis technique could be applied to satellite data in the 10-11 μm region and television imagery, the 6.7 μm observations are considered more suited to a moisture analysis since the emission is a function of moisture content in the mid-troposphere. One can also expect that satellite

*See Fig. 8b for an indication of the availability of conventional radiosonde observations.

spectrometric observations such as those described by Conrath (1969) and Smith and Howell (1971) will continue to improve and become more frequently available as improved sensors are flown on future satellites. It is clear that these values will be more quantitative and an improvement over what is described here. However, until that time, and even beyond, it is felt that this spatially contiguous coverage prepared in easily-handled photofacsimile form from the THIR data can be of substantial utility in the study of upper tropospheric dynamics and water vapor transport.

The global derived wind flow analysis, shown in Fig. 8(a) was achieved by using the 6.7 μm data in Fig. 6 and the technique described in Section 4(b). The equator-crossing times are shown for the satellite orbits in Fig. 8(a). Corresponding 400 mb wind observations were plotted for broader synoptic time periods in Fig. 8(b). A comparison of the results in these two figures revealed generally good agreement. Table 2 shows a quantitative comparison of 6.7 μm-derived wind direction and wind directions at various levels for 145 stations listed in the Hemispheric Weather Data Tabulations, available from the National Climatic Data Center, Asheville, North Carolina.

As can be readily seen, the 400 mb level has the highest percentage of derived wind directions within 0-10° of conventional winds and the lowest percentage of mean departure from conventional observations. This is consistent with the fact that the principal portion of the emission observed in the 6.7 μm region occurs, on the average nearest the 400 mb level (Fig. 2(a)). However, the

Table 2

Derived Wind Direction vs Observed Wind Direction

Level	No. of Samples	Mean Departure	Frequency of Occurrence (%) (Departure of Observed from Derived)									
			0-10°	11-20°	21-30°	31-40°	41-50°	51-60°	61-70°	71-80°	81-90°	>90°
700 mb	143	42.41°	21.0	19.6	12.6	6.3	9.8	5.6	8.4	0.7	2.8	13.3
600 mb	43	37.98°	32.6	18.6	11.6	2.3	4.7	7.0	4.7	2.3	2.3	14.0
500 mb	145	25.90°	39.3	17.9	11.7	10.3	6.9	4.8	2.1	2.1	0	4.8
400 mb	143	22.60°	46.2	15.4	12.6	8.4	4.2	6.3	0	2.1	2.1	2.8
300 mb	136	25.46°	44.9	18.4	10.3	6.6	4.4	4.4	2.2	1.5	1.5	5.9
200 mb	125	35.18°	33.6	22.4	8.8	5.6	5.6	4.8	4.0	3.2	1.6	10.4

NOTE: Samples were selected wherever a derived wind direction was available over a land station observation point.

patterns seen on the photofacsimile film strips are influenced by water vapor at levels somewhat removed from 400 mb, depending primarily on whether the upper atmosphere is drier or more moist than normal. In general, the derived wind flow should be considered to be representative of a layer ranging between 250 and 500 mbs.

One typical problem was revealed in obtaining the analysis shown in Fig. 8(a). In three instances, the derived wind direction departed 180° from the wind direction observed by conventional means. One of these instances occurred over the Yugoslav-Bulgarian-Caspian Sea region where a strong wind shear can be seen in Fig. 8(b). Another area was located in the Atlantic Ocean between 30°-60°W and 25°-35°N, where the indicated southeasterly winds were inferred to be northwesterly winds. This error would not have occurred had the analyst been aware of the existing wind flow patterns based on the conventional radiosonde data. In addition, the information gained from the 6.7 μm imagery can be considered to more rigorously define the 400 mb wind flow when used to supplement an analysis of conventional data rather than to replace it.

The greatest utility of the 6.7 μm imagery occurs in deriving wind flow in non-cloudy regions. In the tropics and remote oceanic regions, it is believed that the procedure outlined here should be a valuable adjunct to cloud motion observations obtained in the visible portion of the electromagnetic spectrum from geostationary satellites such as the Applications Technology Satellites (ATS-I and III).

4. SUMMARY

Some examples have been discussed which show that the water vapor channel imagery from meteorological satellites, particularly Nimbus 4, can be quite helpful in improving moisture and wind analyses. The satellite imagery permits the extrapolation of conventional measurements into data sparse regions so that much greater detail can be introduced into analyses of these parameters. These analyses suggest that water vapor would be of particular help over the oceanic regions where conventional data is very sparse. In addition, the large area, synoptic coverage afforded by the satellite, in conjunction with these water vapor data should be helpful in providing insight as to the interconnection of tropical and mid-latitude systems which are manifested in the upper troposphere.

REFERENCES

Allison, L. J., 1964: An Analysis of TIROS II Radiation Data Recorded over New Zealand at Night, NASA Technical Note D-1910, pp. 17.

Allison, L. J., and G. Warnecke, 1965: The Interpretation of TIROS Radiation Data for Practical Use in Synoptic Weather Analysis, NASA Technical Note D-2851, National Aeronautics and Space Administration, Washington, D.C. pp. 28.

Beran, D., E. Merrit, and D. Chang, 1968: Interpretation of Baroclinic Systems and Wind Fields as Observed by the Nimbus II MRIR. Final Report, Contract NAS 5-10334, Allied Research Associates, Concord, Mass., 135 pp.

Conrath, B. J., 1969: On the estimation of relative humidity profiles from medium resolution infrared spectra obtained from satellite. J. Geophys. Res., 74, 3347-3361.

Keegan, T. J., 1972: An evaluation of direct readout infrared data. Monthly Weather Review, 100, 117-125.

Martin, F. L., and V. V. Salomonson, 1970: Statistical characteristics of subtropical jet stream features in terms of MRIR observations from Nimbus II. Journal of Applied Meteorology, 9, 508-520.

McCulloch, A. W., 1970: The temperature-humidity infrared radiometer (THIR) experiment. The Nimbus IV User's Guide, Goddard Space Flight Center, Greenbelt, Md., pp. 25-63.

Möller, F., and E. Raschke, 1969: Problems of Meteorological observations from satellites. Space Science Reviews, 9, 90-148.

Nordberg, W., A. W. McCulloch, L. L. Foshee, and W. R. Bandeen, 1966: Preliminary results from Nimbus II. Bulletin of the American Meteorological Society, 11, 857-872.

Raschke, E., and W. R. Bandeen, 1967: A quasi-global analysis of tropospheric water vapor content from TIROS IV radiation data. Journal of Applied Meteorology, 6, 468, 481.

Shenk, W. E., and V. V. Salomonson, 1970: Visible and infrared imagery from meteorological satellites. Applied Optics, 9, 1747-1760.

Smith, W. L. and H. B. Howell, 1971: Vertical distribution of water vapor from satellite infrared spectrometer measurements, J. Appl. Meteorol., 1026-1034.

FIGURE CAPTIONS

Figure 1. Nimbus 4 THIR photofacsimile imagery in the 6.7 and 11.5 μm spectral regions at local midnight over the Western United States on orbit 2565, 16 October 1970. Area A is a cloud mass visible in both spectral regions. Areas B and C are regions that are clear in the 11.5 μm observations but show very noticeable detail in the 6.7 μm observations.

Figure 2(a). A plot of the function ψ, showing the atmospheric emission contribution at various altitudes to the radiance observed in the Nimbus 4 THIR 6.7 μm channel.

2(b). The spectral response of the Nimbus 4 THIR, 6.7 μm channel.

Figure 3(a). Analysis of conventional 400 mb radiosonde data at 1200 GMT, 16 October 1970 over the United States. Mixing ratio is in g/kgm.

3(b). Enhanced 400 mb moisture analysis over the United States at 1200 GMT, 16 October 1970. The light to dark grey patterns of moisture from the 6.7 μm data in Figure 1, orbit 2565, 16 October 1970 at 0830 GMT was integrated into the conventional radiosonde moisture data. The light grey patterns indicate water vapor emission generally from the 700 mb to 200 mb level.

Figure 4. A comparison of (a) Nimbus 4 THIR 6.7 μm imagery on orbit 2565, 16 October 1970 and (b) a detailed streamline analysis derived from the patterns shown in part (a) and conventional wind observations over the Western U.S. The arrowheads shown in part (b) were inferred from the light and dark patterns in part (a) that result from upper tropospheric dynamics affecting the distribution of water vapor.

Figure 5. Composite of photofacsimile film strips (6.7 μm channel) Nimbus 4 THIR, orbits 2561 to 2574 (night), 16 October 1970.

Figure 6. Mercator projection of 5 shades of grey of 6.7 μm data, Nimbus 4 THIR, orbits 2561 to 2574 (night), 16 October 1970 using Fig. 5 as the data base.

Figure 7. Enhanced global 400 mb chart of moisture content (mixing ratio, in g/kg) 00 GMT 16 October 1970 to 00 GMT 17 October 1970, using 6.7 μm and conventional 400 mb radiosonde moisture data.

Figure 8(a). Derived global mid-tropospheric wind flow, approx. 01 to 20 GMT, 16 October 1970, using 6.7 μm data from Figure 6 and technique described in Section 4(b).

8(b). Conventional 400 mb wind measurements from 00, 12 GMT 16 October 1970 and 00 GMT 17 October 1970 observations.

NIMBUS 4 THIR
16 OCTOBER 1970
ORBIT 2565 (N)

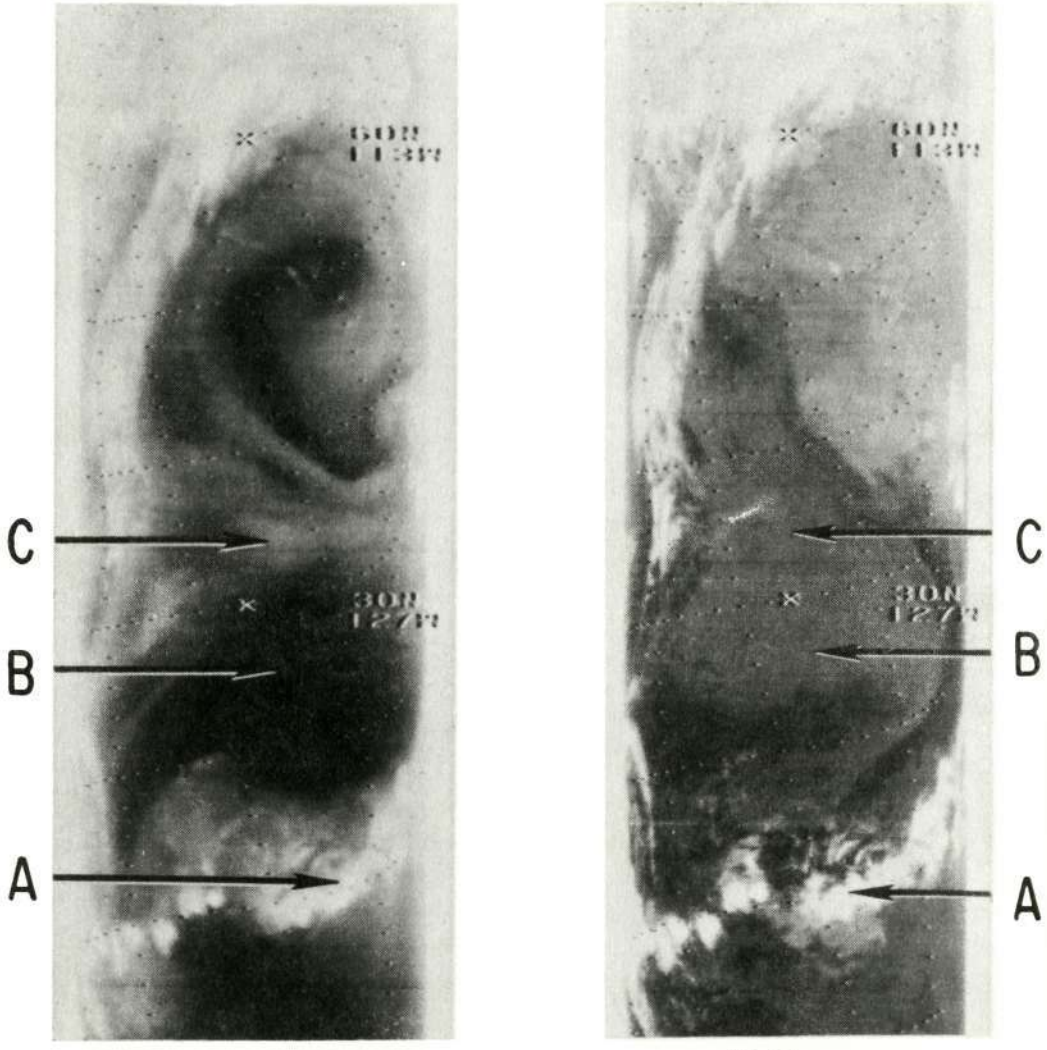

6.7μm WATER VAPOR CHANNEL

11.5μm WINDOW CHANNEL

Fig. 1

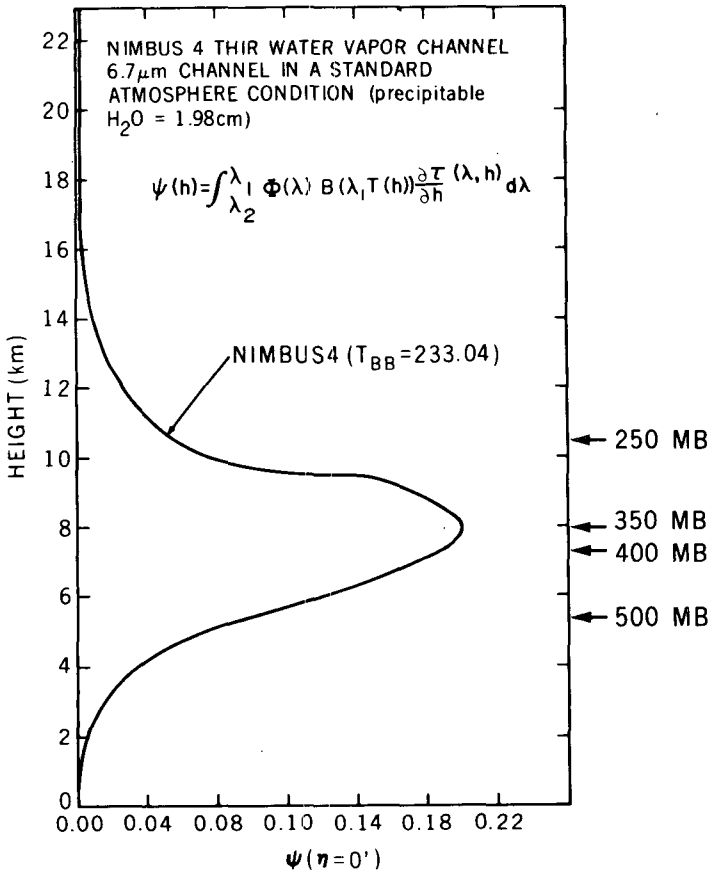
NIMBUS 4 THIR WATER VAPOR CHANNEL
6.7μm CHANNEL IN A STANDARD
ATMOSPHERE CONDITION (precipitable
H2O = 1.98cm)
ψ(h)=∫λ1 λ2 Φ(λ) B(λ,T(h))∂τ/∂h (λ,h) dλ
NIMBUS4 (TBB=233.04)
250 MB
350 MB
400 MB
500 MB
HEIGHT (km)
0 2 4 6 8 10 12 14 16 18 20 22
0.00 0.04 0.08 0.10 0.14 0.18 0.22
ψ(η=0')

(a)

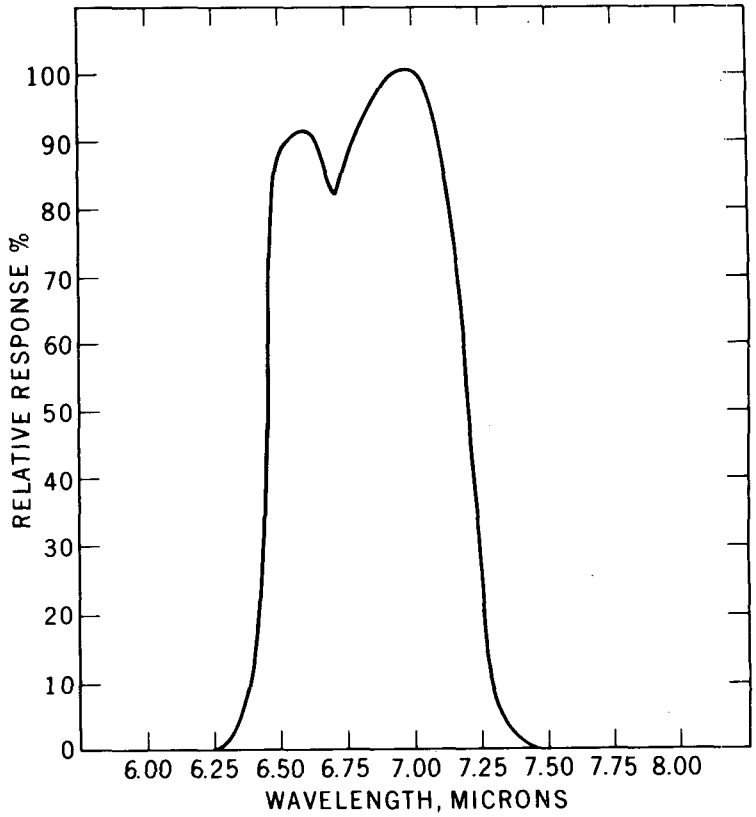
RELATIVE RESPONSE %
0 10 20 30 40 50 60 70 80 90 100
6.00 6.25 6.50 6.75 7.00 7.25 7.50 7.75 8.00
WAVELENGTH, MICRONS

(b)

Fig. 2

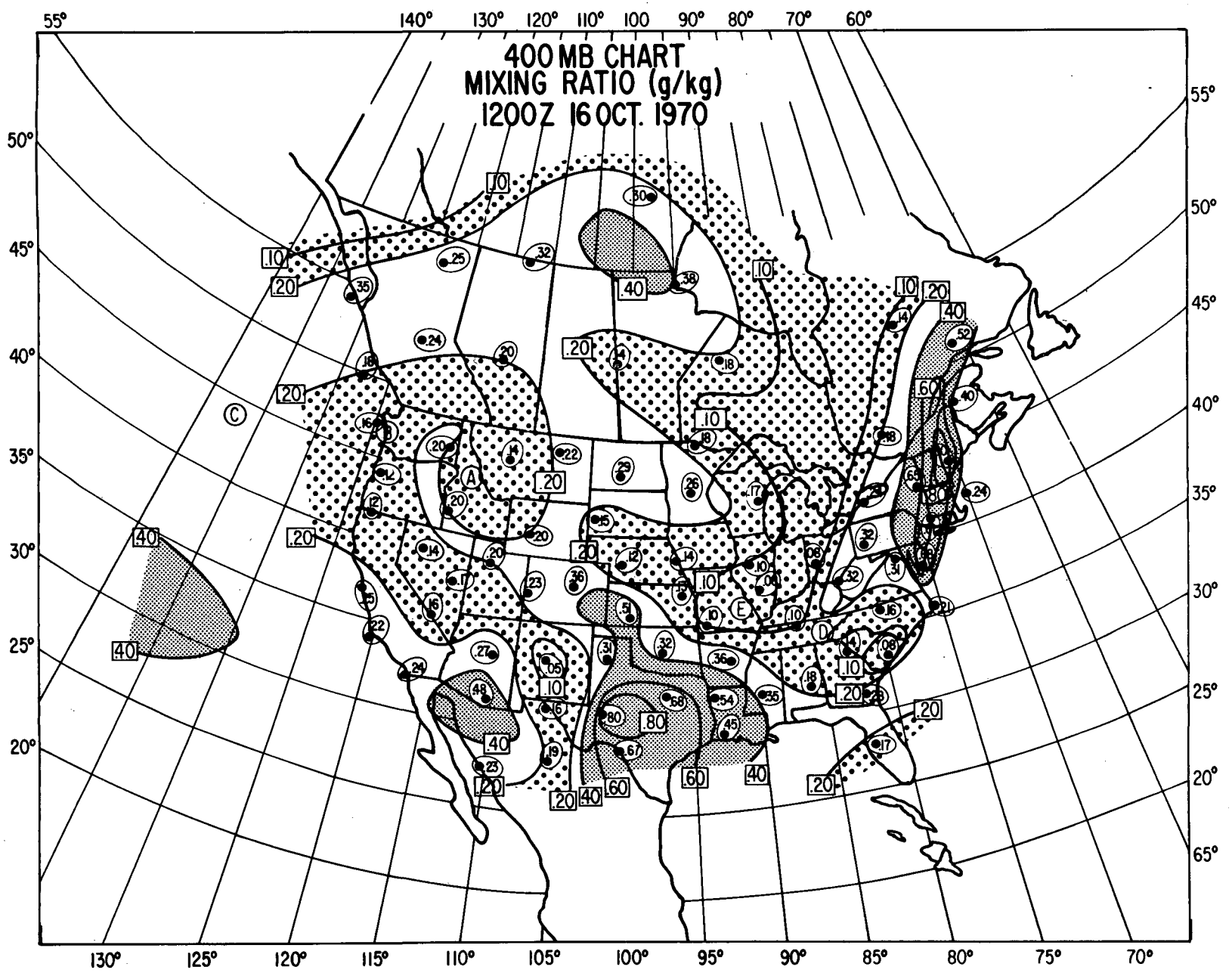
400 MB CHART
MIXING RATIO (g/kg)
1200Z 16 OCT. 1970
55°
140°
130°
120°
110°
100
90°
80°
70°
60°
50°
45°
40°
35°
30°
25°
20°
65°
130°
125°
120°
115°
110°
105°
100°
95°
90°
85°
80°
75°
70°
A
C
D
E

Fig. 3(a)

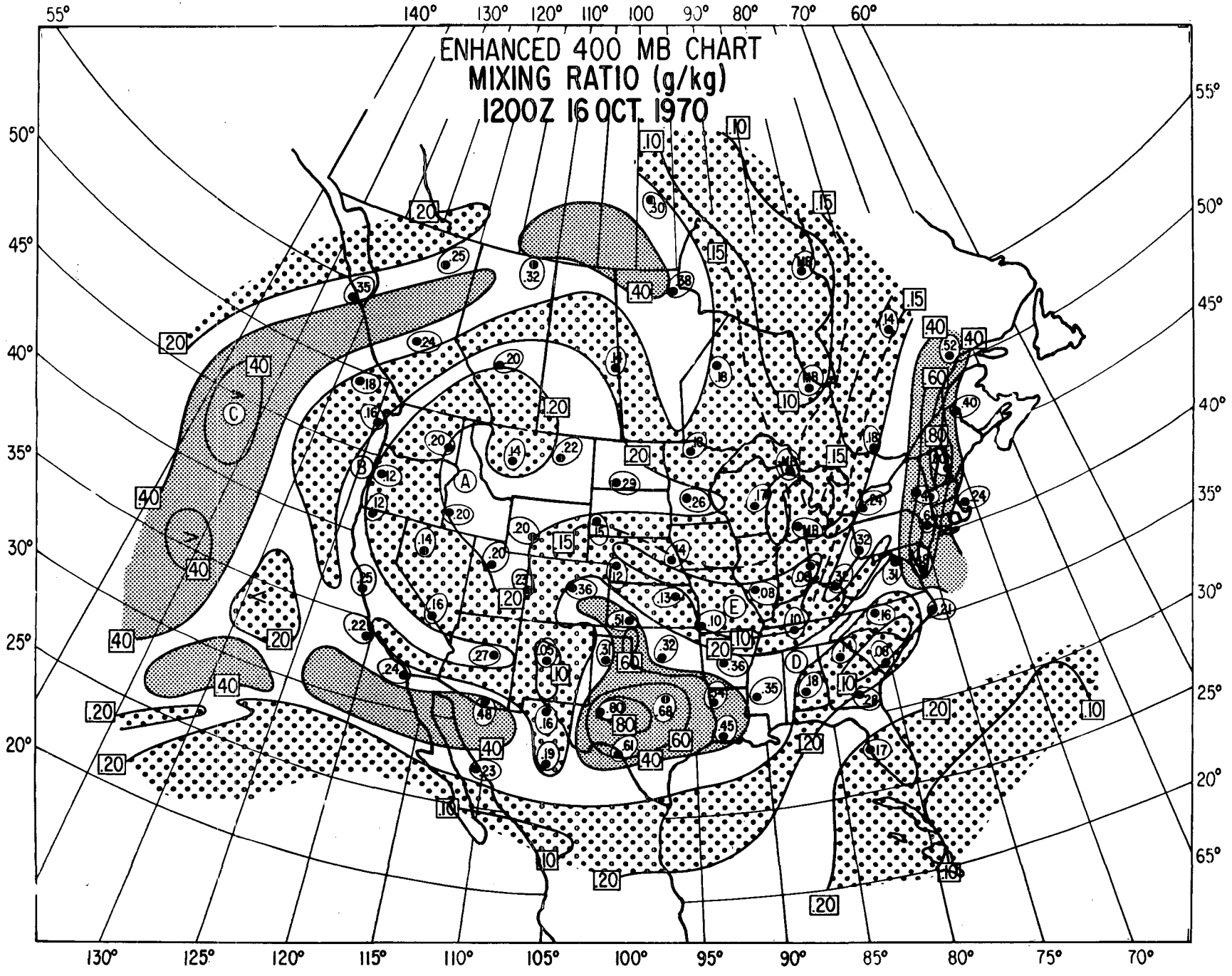
ENHANCED 400 MB CHART
MIXING RATIO (g/kg)
1200Z 16 OCT. 1970
A
B
C
D
E

Fig. 3(b)

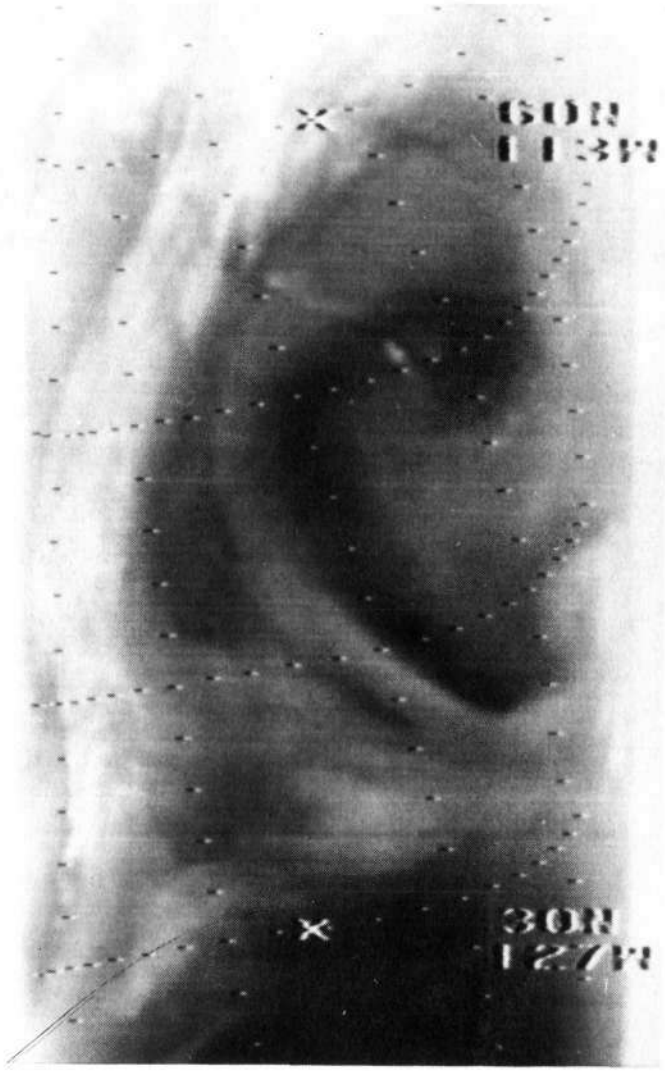

NIMBUS 4 THIR (6.7μ)
ORBIT 2565 (N)
16 OCTOBER 1970

DERIVED STREAMLINE
ANALYSIS

Fig. 4

16 OCTOBER 1970

6.7

Fig. 5

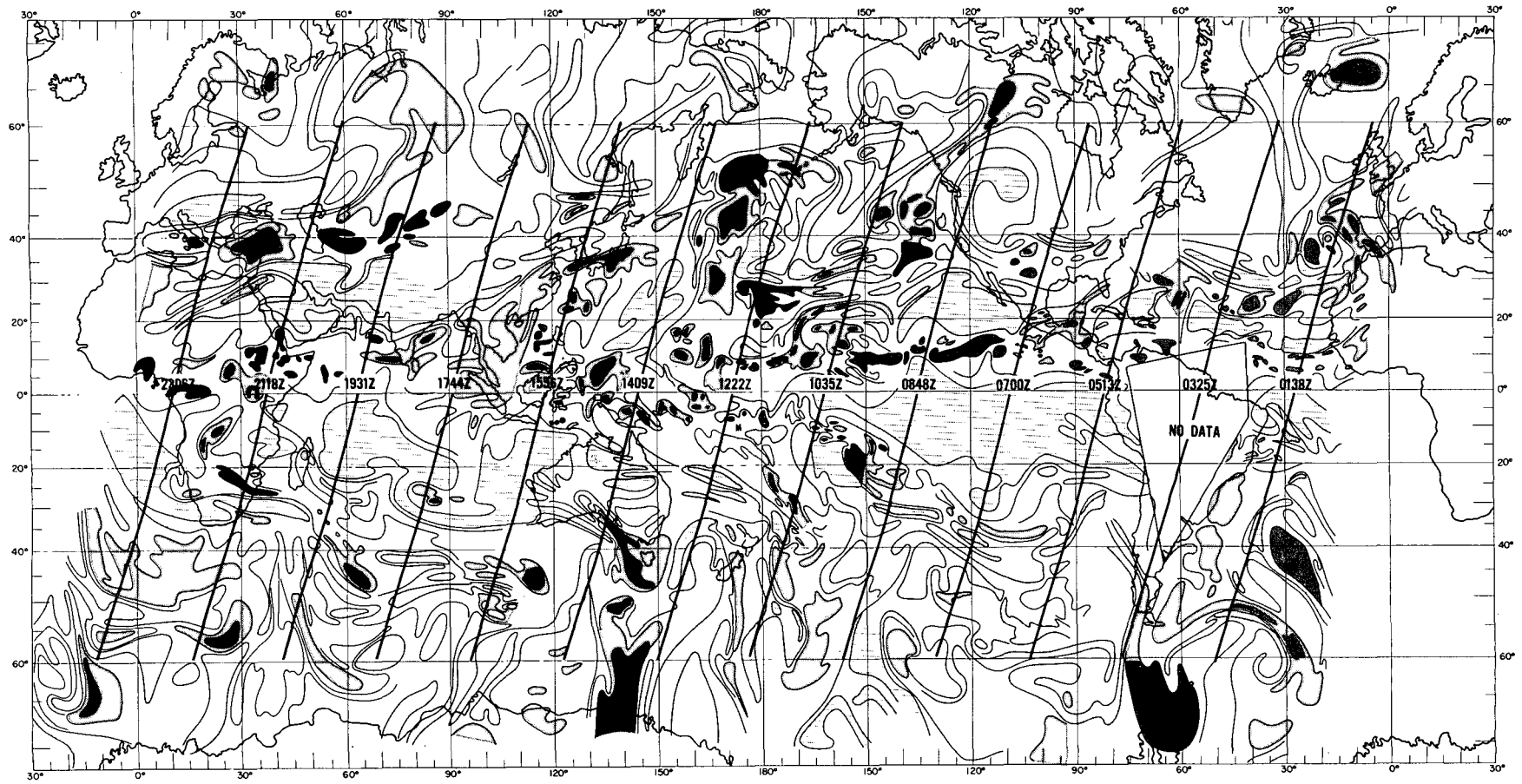

DEPICITION OF NIMBUS 4 THIR
6.7μm IMAGERY
ORBITS 2561 (N) TO 2574 (N)
16 OCT., 1970

FIGURE 6

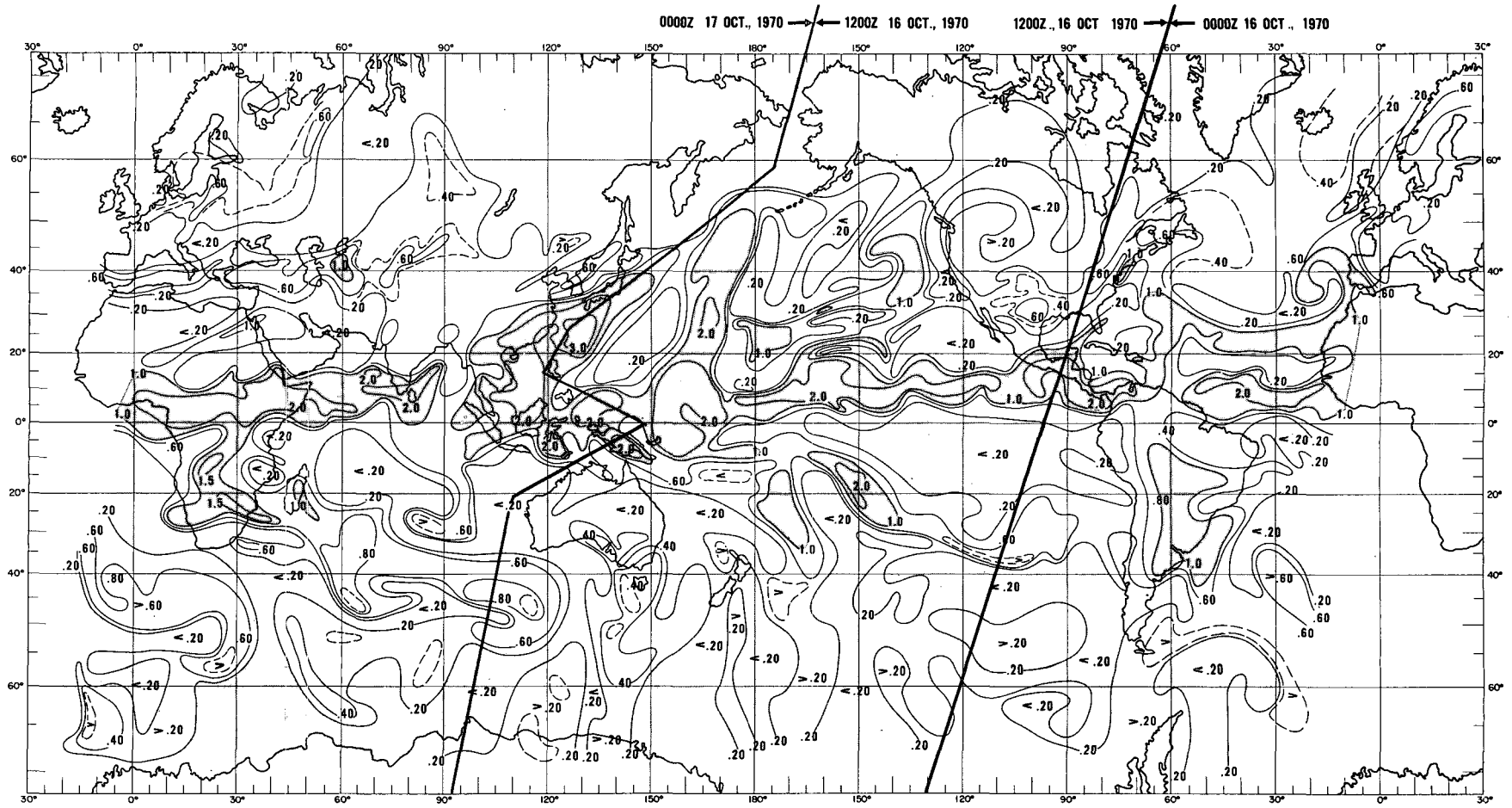
0000Z 17 OCT., 1970
1200Z 16 OCT., 1970
1200Z., 16 OCT 1970
0000Z 16 OCT., 1970
ENHANCED 400 MB CHART
MIXING RATIO (g/kg)
0000Z 16 OCT.–000Z 17 OCT., 1970
.20 g/kg and <
1.0 g/kg and >

FIGURE 7

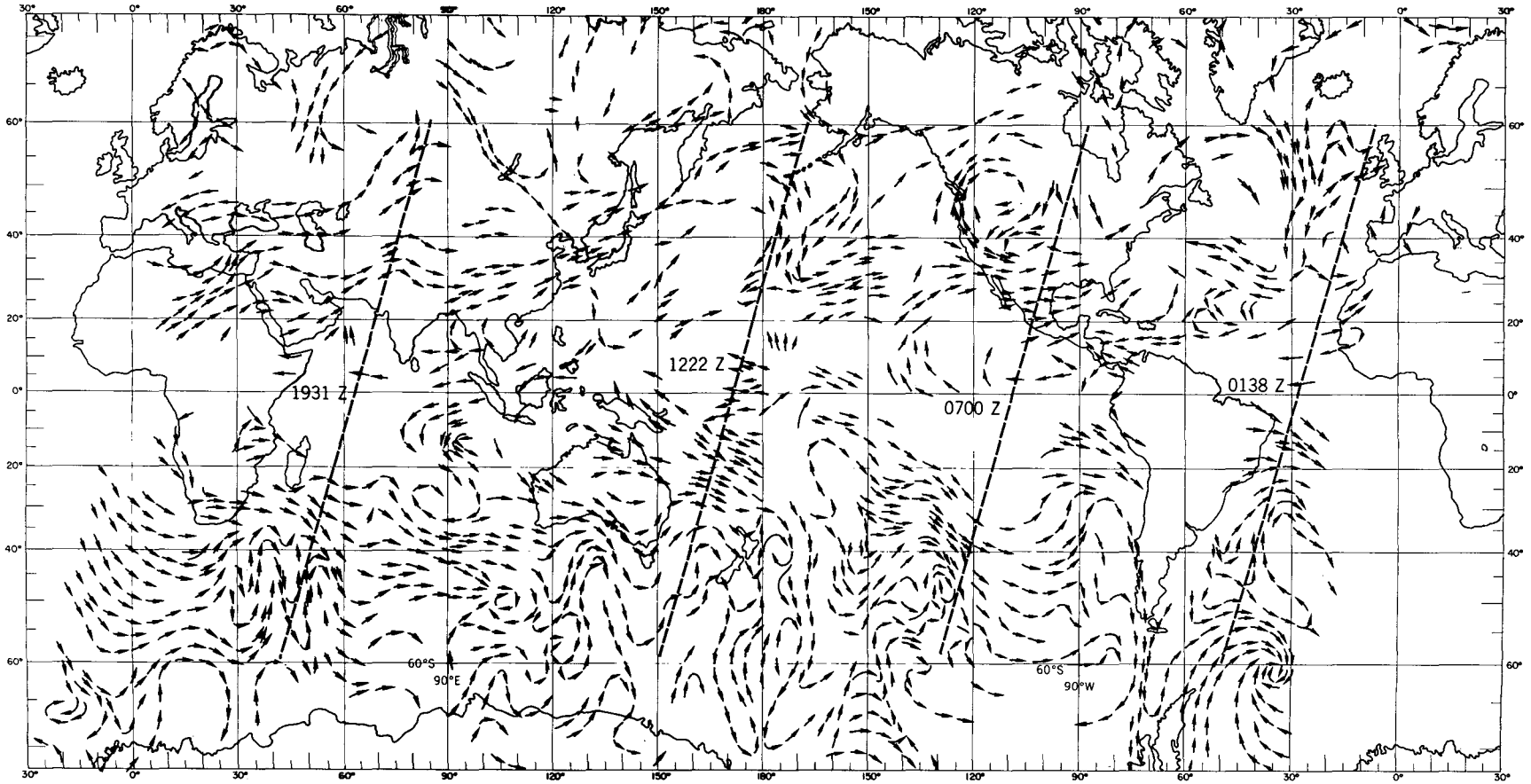

DERIVED MID-TROPOSPHERIC WIND FLOW
16 OCTOBER 1970

Fig. 8(a)

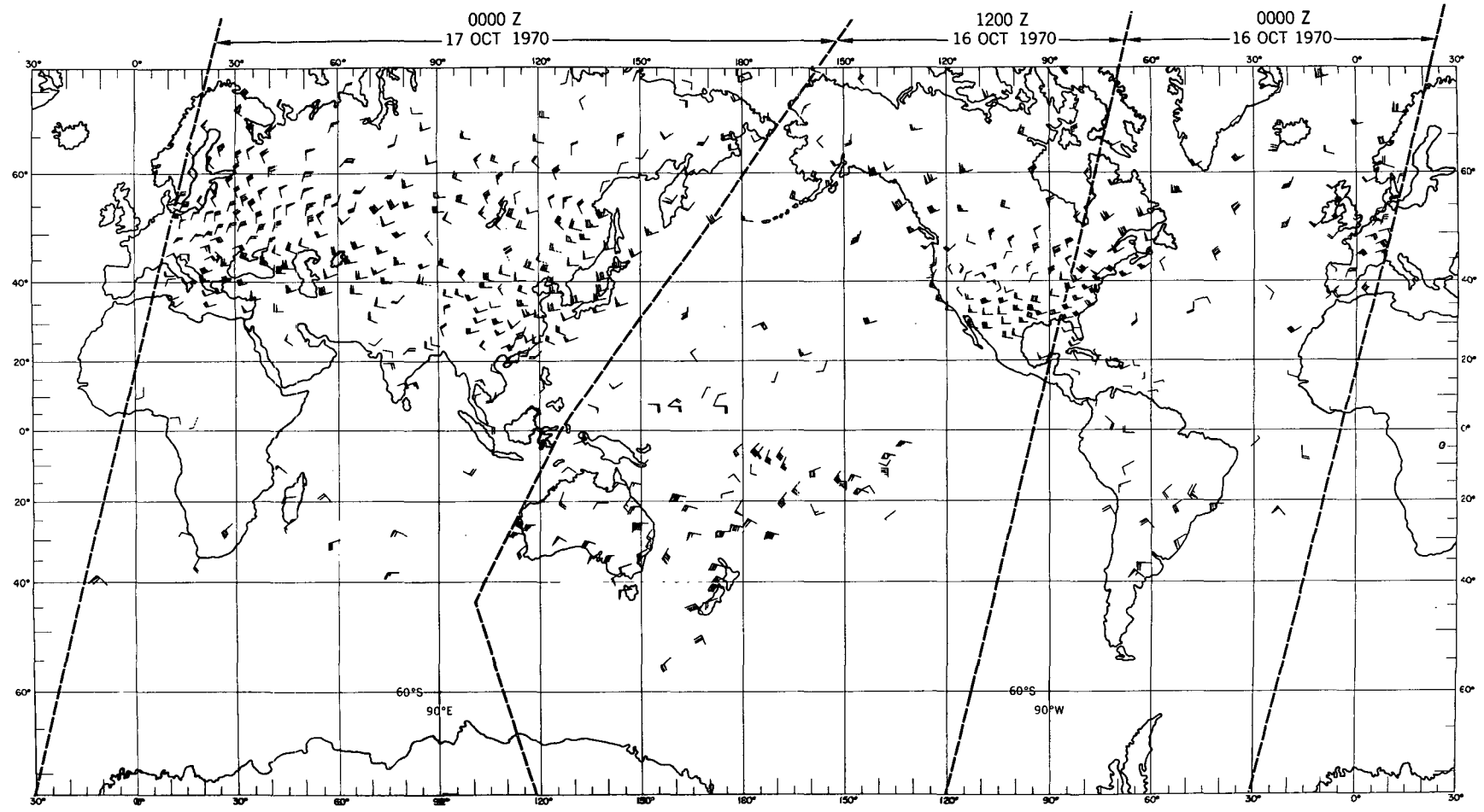
0000 Z
17 OCT 1970
1200 Z
16 OCT 1970
0000 Z
16 OCT 1970
60°S
90°E
60°S
90°W

Fig. 8(b)